Single-Molecule Electronics

DOI: 10.1002/ange.201104757

# Influence of the Chemical Structure on the Stability and Conductance of Porphyrin Single-Molecule Junctions**

*Mickael L. Perrin, Ferry Prins, Christian A. Martin, Ahson J. Shaikh, Rienk Eelkema, Jan H. van Esch, Tomas Briza, Robert Kaplanek, Vladimir Kral, Jan M. van Ruitenbeek, Herre S. J. van der Zant, and Diana Dulić**

The use of porphyrin molecules as building blocks of functional molecular devices has been widely investigated.[1,2] The structural flexibility and well-developed synthetic chemistry of porphyrins allows their physical and chemical properties to be tailored by choosing from a wide library of macrocycle substituents and central metal atoms. Nature itself offers magnificent examples of processes that utilize porphyrin derivatives, such as the activation and the transport of molecular oxygen in mammals and the harvesting of sunlight in plant photosynthetic systems. In order to exploit the highly desirable functionality of porphyrins in artificial molecular devices, it is imperative to understand and control the interactions that occur at the molecule–substrate interface. Such interactions largely depend on the electronic and conformational structures of the adsorbed molecules, which can be studied using techniques such as scanning tunneling microscopy,[3–7] UV photoemission spectroscopy,[8] and X-ray photoemission spectroscopy,[2] and on a theoretical level with density functional calculations.[9] Recent studies on conjugated rod-like molecules have shown that molecular conductance measurements can be significantly affected by the binding geometry,[10] coupling of the π orbitals to the leads,[11] or π–π stacking between adjacent molecules.[12] Herein, we present the results of a study of the interaction of laterally extended π-conjugated porphyrin molecules with electrodes by means of time- and stretching-dependent conductance measurements on molecular junctions. We further investigate strategies to reduce interactions of the molecular π electrons with the metal electrodes by modifying the chemical structure of the porphyrin molecules.

We used the series of molecules represented in Figure 1 a–c to examine the influence of the molecular structure on the formation of porphyrin single-molecule junctions. Since the thiol group is most commonly used to contact rod-like molecules to form straight molecular bridges,[13] we first compared 5,10,15,20-tetraphenylporphyrin without thiol termination ($H_2$-TPP; Figure 1 a) to a nearly identical molecule with two thiol groups on opposite sides of the molecule (5,15-di(*p*-thiophenyl)-10,20-di(*p*-tolyl)porphyrin ($H_2$-TPPdT); Figure 1 b). To investigate the influence of the molecular backbone geometry on the junction formation we further studied a thiol-terminated porphyrin molecule with two bulky pyridine axial groups attached through an octahedral $Ru^{II}$ ion ($[Ru^{II}${5,15-di(*p*-thiophenyl)-10,20-diphenylporphyrin}$(py)_2]$ (Ru-TPPdT); Figure 1 c). As a consequence of steric hindrance, the pyridine groups in Ru-TPPdT reduce the direct interaction of the metal electrodes with the π face of the porphyrin. A similar strategy was used previously.[4]

Prior to electrical characterization, the molecules were deposited using self-assembly from solution. To study the conductance of these molecules we used lithographic mechanically controllable break junctions (MCBJs) in vacuum at room temperature. The layout of an MCBJ device in a three-point bending mechanism is shown in Figure 1 d. Details concerning the synthesis of the molecules and the experimental procedures are given in the Supporting Information. Sets of 1000 consecutive breaking traces from individual junctions were analyzed numerically to construct "trace histograms" of the conductance ($\log_{10} G$ versus the electrode displacement $d$).[14,15] This statistical method maps the breaking dynamics of the junctions beyond the point of rupture of the last monatomic gold contact (defined as $d = 0$), which has a conductance of one quantum unit $G_0 = 2e^2/h$. Areas of high counts represent the most typical breaking behavior of the molecular junctions. Figure 2 presents trace histograms as well as examples of individual breaking traces for acetone as reference, $H_2$-TPP, $H_2$-TPPdT, and Ru-TPPdT. For all three porphyrin molecules as well as for the reference sample several junctions were measured (see the Supporting Information). Herein, we only show a typical set of junctions.

In the junction which was exposed to pure acetone (Figure 2 a), the Au bridge initially gets stretched until a plateau around the conductance quantum ($G \approx G_0$) is observed (only visible in the individual traces shown in

[*] M. L. Perrin, F. Prins, Dr. C. A. Martin, Prof. Dr. H. S. J. van der Zant, Dr. D. Dulić
Kavli Institute of Nanoscience, Delft University of Technology
Lorentzweg 1, 2628 CJ Delft (The Netherlands)
E-mail: d.dulic@tudelft.nl
A. J. Shaikh, Dr. R. Eelkema, Prof. Dr. J. H. van Esch
Department of Chemical Engineering
Delft University of Technology (The Netherlands)
Dr. T. Briza, Dr. R. Kaplanek, Prof. Dr. V. Kral
Institute of Chemical Technology, Prague (Czech Republic)
Prof. Dr. J. M. van Ruitenbeek
Kamerlingh Onnes Laboratory, Leiden University (The Netherlands)

[**] This research was carried out with financial support from the Dutch Foundation for Fundamental Research on Matter (FOM) and the VICI (680-47-305) grant from The Netherlands Organisation for Scientific Research (NWO). We would like to thank Prof. Dr. Robert Metzger and Dr. Graeme R. Blake for careful reading of the manuscript.

Supporting information for this article is available on the WWW under http://dx.doi.org/10.1002/anie.201104757.

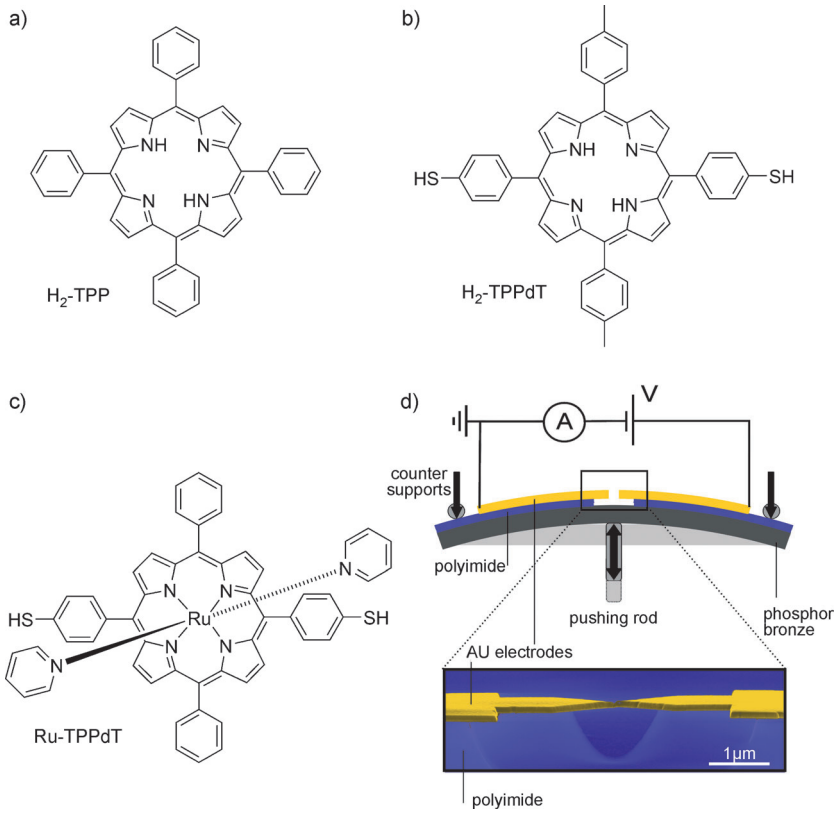


***Figure 1.*** Structures of a) $H_2$-TPP, b) $H_2$-TPPdT, c) Ru-TPPdT. d) Top: layout of an MCBJ. Bottom: scanning electron micrograph of an MCBJ device (colorized for clarity). From the scale bar it is clear that the suspended part of the electrode bridge is about 1.5 µm long.

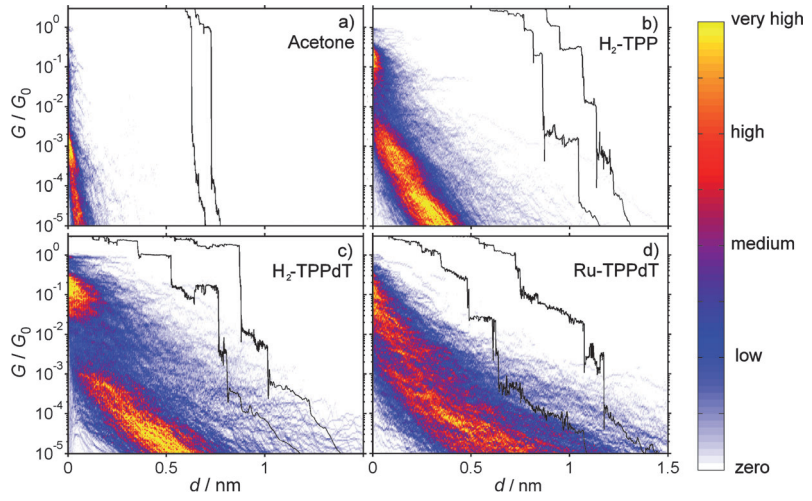


***Figure 2.*** Trace histograms constructed from 1000 breaking traces for junctions exposed to pure acetone, $H_2$-TPP, $H_2$-TPPdT, and Ru-TPPdT. The black curves are examples of individual breaking traces (offset for clarity). For the construction of the histograms, $d = 0$ for each curve was set to the point where the conductance drops sharply below 1 $G_0$. All histograms were taken at a bending speed of 30 µm s$^{-1}$ (on the scale of the electrodes, this bending is translated into a stretching on the order of 1.8 nm s$^{-1}$) and a bias voltage of 150 mV. No data selection schemes were utilized. For additional trace histograms see the Supporting Information. For (a) we found a decay constant of 2 Å$^{-1}$.

black), which corresponds to a monatomic contact.[14] Upon further stretching, the Au–Au contact is broken and the conductance decreases abruptly to about $10^{-3}$ $G_0$. Beyond this point, electron tunneling between the electrodes leads to a fast conductance decay with stretching (visible as the orange tail), as expected for tunneling across a vacuum barrier.

In contrast, introducing the porphyrin molecules on the junctions leads to pronounced plateaus at different conductance values in the sub-$G_0$ regime. These plateaus can be flat or sloped.[10,16] The representative breaking traces that are included in Figure 2b–d display a set of such plateaus. Averaging over 1000 traces does not lead to a narrow region of high counts in the histograms, in contrast to measurements on rod-like molecules.[14–17] In the trace histogram of $H_2$-TPP (Figure 2b), however, there are two distinct regions with high counts; a high-conductance region (HCR) around $10^{-1}$ $G_0$, and a sloped low-conductance region (LCR) below $10^{-3}$ $G_0$. For $H_2$-TPPdT (Figure 2c), both the HCR and LCR are longer than for $H_2$-TPP; thus, adding the thiol end groups to $H_2$-TPP increases the plateau length, and it reduces the slope of the LCR. In Ru-TPPdT (Figure 2d), the HCR and LCR cannot be distinguished anymore: only one long region sloping from $10^{-1}$ $G_0$ to $10^{-5}$ $G_0$ is present, which has a shallower slope compared to the histograms of $H_2$-TPP and $H_2$-TPPdT, and an increased length.

Additional information about molecular junction configurations can be gained by measuring the evolution of the junction conductance over large time intervals at fixed electrode distances.[18] To obtain such "time traces", we opened the junction in small steps using a servomotor at 77 K. At this low temperature, the surface diffusion is reduced, which enhances the stability without causing extensive changes in the molecular conductance.[19] We then measured the conductance in the range from 1 $G_0$ to $10^{-4}$ $G_0$ at various fixed electrode spacings and for time periods exceeding several hours. As a consequence of the exceptional control over the electrode separation in the MCBJ,[18,19] conductance jumps in these measurements can be attributed to reconfigurations of the molecule in the junction rather than mechanical interference of the setup.

Typical time traces of junctions exposed to pure acetone, $H_2$-TPP, $H_2$-TPPdT, and

Ru-TPPdT are presented in Figure 3. As can be seen in Figure 3a, a stable contact is formed at 1 $G_0$ in the clean junction. A slight increase in the electrode spacing leads to

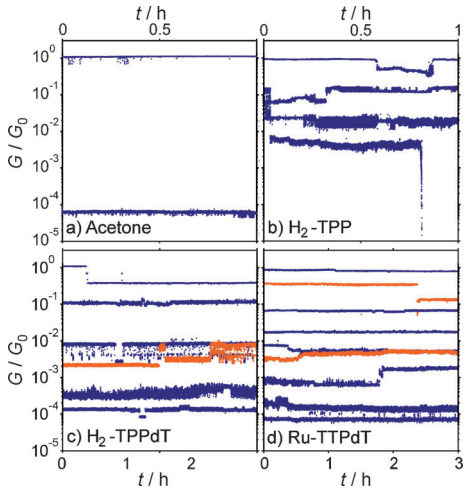


***Figure 3.*** Conductance-versus-time plots for acetone, $H_2$-TPP, $H_2$-TPPdT, and Ru-TPPdT taken at a bias voltage of 150 mV. The traces originate from the same opening event and are taken at intervals of 50 pm. Several lines are displayed in orange for clarity.

abrupt breaking of the contact to a conductance value around $10^{-4}$ $G_0$. In contrast, the presence of porphyrin molecules leads to the formation of junctions with conductances in the region between 1 $G_0$ and $10^{-3}$ $G_0$ (Figure 3b–d). Below $10^{-3}$ $G_0$, the $H_2$-TPP molecule (Figure 3b) exhibits a sudden conductance drop to below $10^{-5}$ $G_0$. In contrast, thiol-terminated $H_2$-TPPdT and Ru-TPPdT (Figure 3c,d) form molecular junctions over the whole range between 1 $G_0$ and $10^{-4}$ $G_0$. The observations support the conclusions drawn from the trace histograms: adding thiol and pyridine groups increases the junction stability and leads to a variety of molecular geometries with different conductance values. To examine the contribution of π stacking of multiple molecules, we measured trace histograms on junctions exposed to 5,10,15,20-tetrakis(3,5-di-*tert*-butylphenyl)porphyrin abbreviated as TBP. As a consequence of the steric hindrance of the butyl groups, the possibility of π stacking between two molecules is reduced. Resulting trace histograms are shown in the Supporting Information. There is no qualitative difference between the trace histogram of TBP and TPP molecules, which demonstrates insignificant influence of π stacking on the formation of different configurations.

A closer inspection of the time traces reveals interesting information on the behavior of the molecule in the junction. Since the electronic noise is much smaller than the width of the bands of the measured conductance values, we conclude that what appears to be noise in the time traces is in fact a sign of small variations in the molecular configuration.[18] Large jumps in the conductance (Figure 3c,d) indicate that a molecular junction can spontaneously change its configuration. In Figure 3c, random telegraph noise between two conductance values is observed indicating the possibility of forming several metastable configurations. Furthermore, Figure 3d shows that a particular junction conductance can be reached from different starting values (blue and orange traces in the middle of the graph).

The presence of a large range of molecular adsorption geometries contrasts with most studies on long rod-like molecules, which typically assume a straight bridging configuration of the molecule with both thiol groups connected to the electrodes (Figure 4a). For $H_2$-TPPdT, such a configuration could be expected. However, the high affinity of the porphyrin π cloud for metal surfaces likely stabilizes other

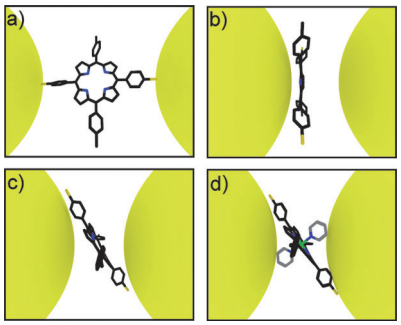


***Figure 4.*** Illustration of four possible configurations of a porphyrin molecule in the junction. a) Bridging configuration, b) STM-like configuration, and c) intermediate configuration of $H_2$-TPPdT; d) intermediate configuration of Ru-TPPdT (pyridine groups shown in gray).

configurations, such as sketched in Figure 4b and c. A stable junction configuration can be formed without thiol groups[20] and recent break junction experiments have demonstrated that benzene moieties can bind directly to gold electrodes.[21,22] Furthermore, it has been reported that the lateral coupling of π orbitals to electrodes influences the single-molecule conductance of rod-like molecular wires.[11,23] Such coupling becomes more likely when laterally extended molecules are probed. In addition, tetraphenylporphyrin molecules have internal degrees of freedom, which can influence the charge transport on a single-molecule level.[24] STM studies indicate that tetraphenylporphyrins can bind to Au(111) through an interaction with their phenyl side groups.[6] On gold surfaces, their conformation can change through rotations of side groups and buckling of the center.[5] Such variations in the adsorption geometry, which can be expected to lead to different conductance values, are likely the origin of the variety of junction configurations that we observe.

In summary, we have demonstrated that porphyrin molecules can form stable bridging molecular junctions even without thiol anchoring groups. Adding thiol end groups and pyridine axial groups to the porphyrin backbone, respectively, increases the stability of the junctions and leads to an increased spread in conductance. This is a result of the formation of different junction configurations. To enable the reliable formation of stable porphyrin junctions, molecules with well-defined adsorption geometries will be required. Quantum chemical calculations could yield more insight into their design as well as the configurations and the conductance of porphyrin single-molecule junctions. Finally, we expect that

multiple junction configurations with considerable variation in the measured conductance values can also be observed for other non-rod-like molecules.

Received: July 8, 2011
Published online: September 28, 2011

**Keywords:** break junctions · molecular electronics · porphyrinoids · single-molecule transport

[1] M. Jurow, A. E. Schuckman, J. D. Batteas, C. M. Drain, *Coord. Chem. Rev.* **2010**, *254*, 2297 – 2310.
[2] S. Mohnani, D. Bonifazi, *Coord. Chem. Rev.* **2010**, *254*, 2342 – 2360.
[3] V. Iancu, A. Deshpande, S.-W. Hla, *Nano Lett.* **2006**, *6*, 820 – 823.
[4] G. Sedghi, K. Sawada, L. J. Esdaile, M. Hoffmann, H. L. Anderson, D. Bethell, W. Haiss, S. J. Higgins, R. J. Nichols, *J. Am. Chem. Soc.* **2008**, *130*, 8582 – 8583.
[5] G. V. Nazin, X. H. Qiu, W. Ho, *Science* **2003**, *302*, 77 – 81.
[6] X. H. Qiu, G. V. Nazin, W. Ho, *Phys. Rev. Lett.* **2004**, *93*, 196806.
[7] J. Brede, M. Linares, S. Kuck, J. Schwöbel, A. Scarfato, S.-H. Chang, G. Hoffmann, R. Wiesendanger, R. Lensen, P. H. J. Kouwer, J. Hoogboom, A. E. Rowan, M. Bröring, M. Funk, S. Stafström, F. Zerbetto, R. Lazzaroni, *Nanotechnology* **2009**, *20*, 275602.
[8] L. Scudiero, D. E. Barlow, U. Mazur, K. W. Hipps, *J. Am. Chem. Soc.* **2001**, *123*, 4073 – 4080.
[9] Z.-L. Cai, M. J. Crossley, J. R. Reimers, R. Kobayashi, R. D. Amos, *J. Phys. Chem. B* **2006**, *110*, 15624 – 15632.
[10] S. Y. Quek, M. Kamenetska, M. L. Steigerwald, H. J. Choi, S. G. Louie, M. S. Hybertsen, J. B. Neaton, L. Venkataraman, *Nat. Nanotechnol.* **2009**, *4*, 230.
[11] I. Diez-Perez, J. Hihath, T. Hines, Z.-S. Wang, G. Zhou, K. Müllen, N. Tao, *Nat. Nanotechnol.* **2011**, *6*, 226.
[12] S. Wu, M. T. González, R. Huber, S. Grunder, M. Mayor, C. Schönenberger, M. Calame, *Nat. Nanotechnol.* **2008**, *3*, 569 – 574.
[13] N. J. Tao, *Nat. Nanotechnol.* **2006**, *1*, 173 – 181.
[14] C. A. Martin, D. Ding, J. K. Sørensen, T. Bjørnholm, J. M. van Ruitenbeek, H. S. J. van der Zant, *J. Am. Chem. Soc.* **2008**, *130*, 13198 – 13199.
[15] M. Kamenetska, M. Koentopp, A. C. Whalley, Y. S. Park, M. L. Steigerwald, C. Nuckolls, M. S. Hybertsen, L. Venkataraman, *Phys. Rev. Lett.* **2009**, *102*, 126803.
[16] A. Mishchenko, D. Vonlanthen, V. Meded, M. Bürkle, C. Li, I. V. Pobelov, A. Bagrets, J. K. Viljas, F. Pauly, F. Evers, M. Mayor, T. Wandlowski, *Nano Lett.* **2010**, *10*, 156 – 163.
[17] M. T. González, S. Wu, R. Huber, S. J. van der Molen, C. Schönenberger, M. Calame, *Nano Lett.* **2006**, *6*, 2238 – 2242.
[18] D. Dulić, F. Pump, S. Campidelli, P. Lavie, G. Cuniberti, A. Filoramo, *Angew. Chem.* **2009**, *121*, 8423 – 8426; *Angew. Chem. Int. Ed.* **2009**, *48*, 8273 – 8276.
[19] C. A. Martin, D. Ding, H. S. J. van der Zant, J. M. van Ruitenbeek, *New J. Phys.* **2008**, *10*, 065008.
[20] E. A. Osorio, M. Ruben, J. S. Seldenthuis, J.-M. Lehn, H. S. J. van der Zant, *Small* **2010**, *6*, 174 – 178.
[21] S. T. Schneebeli, M. Kamenetska, Z. Cheng, R. Skouta, R. A. Friesner, L. Venkataraman, R. Breslow, *J. Am. Chem. Soc.* **2011**, *133*, 2136 – 2139.
[22] S. Martın, I. Grace, M. R. Bryce, C. Wang, R. Jitchati, A. S. Batsanov, S. J. Higgins, C. J. Lambert, R. J. Nichols, *J. Am. Chem. Soc.* **2010**, *132*, 9157 – 9164.
[23] W. Haiss, C. Wang, I. Grace, A. S. Batsanov, D. J. Schiffrin, S. J. Higgins, M. R. Bryce, C. J. Lambert, R. J. Nichols, *Nat. Mater.* **2006**, *5*, 995 – 1002.
[24] M. Ruben, A. Landa, E. Lörtscher, H. Riel, M. Mayor, H. Görls, H. B. Weber, A. Arnold, F. Evers, *Small* **2008**, *4*, 2229 – 2235.

  